Pergamon

Int. J. Solids Structures Vol. 32, No. 6/7, pp. 925–938, 1995

0020–7683/95 $9.50 + .00

0020–7683(94)00169–3

ON THE FAILURE MODE TRANSITIONS IN POLYCARBONATE UNDER DYNAMIC MIXED-MODE LOADING

K. RAVI-CHANDAR
Department of Mechanical Engineering, University of Houston, TX 77204-4792, U.S.A.

(*Received* 1 *February* 1994; *in revised form* 11 *May* 1994)

Abstract—Polycarbonate is known to exhibit rate dependent inelastic behavior. In the present work, it is shown that under predominantly mode II loading, superposed with a hydrostatic compressive stress field, the rate dependence manifests itself in interesting failure mode transitions from ductile to brittle to ductile again. The second transition is quite unusual and is examined in light of the hydrostatic compression and thermal softening of the material.

1. INTRODUCTION

Dynamic fracture investigations over the past two decades have concentrated on obtaining the dynamic crack growth criterion under mode I loading conditions. The focus on mode I loading is usually justified by considering that under mixed-mode or pure mode II loading, the crack will quickly find the path along which the local conditions are of the mode I type. This is, in fact, a generalization of the ideas of Erdogan and Sih (1963) and Cotterell and Rice (1980). Experimental observations of dynamically curving cracks under mixed-mode loading reinforce this impression, although in some experiments cracks were observed to propagate along a straight line under mixed-mode loading [see for example Ravi-Chandar and Knauss (1984)]. While inertia effects may play a role in determining the path evolution and crack speed, the mechanisms of fracture, as observed from the crack surface morphology, were clearly similar to that observed under mode I crack propagation. It appears that the mode I type of crack growth possesses the fracture mechanism with the lowest energy requirement for crack growth. Broberg (1983) showed, particularly with respect to geological fractures where a mean pressure load is superposed on the shearing loads, that if the in-plane compression is sufficiently large, the only available path for crack extension might be along the direction of maximum shear and that while experimentally difficult, "mode II growth should be obtained for virtually all materials", the reasoning being that any micro cracks that are formed ahead of the crack will be closed by the compressive stresses. While not quite obvious, the energy required for this kind of crack growth should be larger than the mode I crack growth.

Kalthoff (1988, 1990) investigated the problem of dynamic fracture under mixed-mode loading using a simple configuration shown in Fig. 1(a). The steel specimen was impacted by a steel projectile traveling at speeds of up to 70 m/s. The crack tip state was followed using a high speed camera and the method of caustics. The caustics were interpreted as indicating a pure mode II state at the crack tip. Kalthoff found that at low impact speeds, a kinked crack propagated from the root of the machined notch and broke the specimen in two pieces, with the kink angle in the range of 70°. This indicated that the maximum hoop stress criterion of Erdogan and Sih (1963) probably governs crack initiation; fracture surface morphology supports this conclusion by revealing that cleavage is the dominant failure mechanism. Above a critical speed, Kalthoff observed that the crack did not kink significantly (only about 10°), and that it arrested after propagating a short distance in spite of the fact that the energy supplied by impacting at a higher projectile speed was higher. Fracture surface morphology indicated that highly localized shear deformation

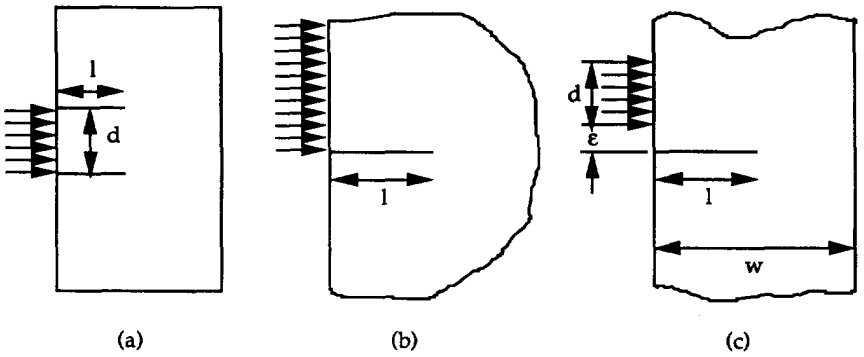

Fig. 1. Impact loading condition for generation of dynamic mixed-mode loading: (a) experimental arrangement of Kalthoff (1988) using two edge cracks; d is the diameter of the projectile and l is the crack length; (b) semi-infinite plate with an edge crack used in the analysis of Lee and Freund (1990); (c) experimental arrangement used in the present work; the distance ε was varied in the experiments to vary the rate of loading.

occurred ahead of the initial crack tip and that the shear mode crack propagated through this shear band.

Lee and Freund (1990) analysed an idealized problem, shown in Fig. 1(b), in an effort to interpret the experimental results of Kalthoff. An elastic half-space containing an edge crack, with an imposed velocity on one side of the crack was considered. The imposed boundary conditions correspond to a traction free stationary crack. The problem was analysed using the elastodynamic theory and the time variation of the stress intensity factors was obtained. A key result of the analysis was the indication that in the idealized problem, in addition to developing a mode II stress intensity K_{II}, a small *negative* mode I stress intensity K_I also developed. In mathematically sharp cracks, the presence of a negative K_I indicates an interpenetration of the upper and lower surfaces of the crack which must be fixed by modifying the crack face boundary conditions to include contact forces; in laboratory cracks with a finite gap, the imposed biaxial loading could lead to a tendency for the two machined cracks to approach each other. Mason *et al.* (1992) indicated that this is indeed the case through experiments using a 1.5 mm thick slot in a PMMA specimen, where the out-of-plane displacement gradients were measured using the coherent gradient sensor technique. The analysis considered a stationary crack in an elastic material and thus the results are applicable only in a short time range after impact of the projectile. Lee and Freund (1990) also showed that the maximum hoop stress occurred at an angle of about 63° during the time interval $t < 3l/C_d$, where l is the length of the crack and C_d is the longitudinal wave speed. Thus, if the failure mechanism is dominated by the maximum stress, one expects a kinked crack initiation as in the low velocity impact experiments of Kalthoff (1988). The linear elastodynamic analysis of Lee and Freund (1990) is, of course, inadequate in addressing the shear cracking at higher impact speeds.

Note that the model problem is an accurate reflection of the experiments of Kalthoff (1988), Mason *et al.* (1992) and the present work only up to $t < \sqrt{(l^2+d^2)}/C_d$; where d is the diameter of the projectile. Beyond this time, the finite extent of the projectile loading will be felt at the crack tip. Thus, in the Kalthoff arrangement, where $l = d$, the analysis is applicable until $t = 1.414l/C_d$. Two key results need to be emphasized. Firstly, the imposed velocity boundary condition produces a compressive mode I stress intensity factor, although the magnitude is significantly smaller than the mode II stress intensity factor. For long times, the experimental results of Mason *et al.* (1992) indicated an increase in the mode II component until about $t = 10l/C_d$, followed by a rapid drop off to zero at about $t = 15l/C_d$, while the compressive mode I component increased rapidly in this same time span. These results are, of course, influenced by the specimen dimensions and perhaps by the impact process. The implication is that the crack initiation angle will be around 63° only if the crack initiation occurs within $t < 3l/C_d$. Secondly, the analysis extracts only the stress intensity factors and thus implicitly assumes that the near tip stress field, up to the onset of

crack initiation, is governed by the square root singular field. We shall explore in the present work, the evolution of the stress field near the crack tip using the method of photoelasticity. Also we will demonstrate fracture mode transitions from ductile to brittle crack kinking to straight shear fracture as a function of the rate of loading in polycarbonate. The micromechanisms responsible for the mode transitions will also be explored.

2. EXPERIMENTAL DETAILS

The specimen geometry and loading configuration are shown in Fig. 1(c). Polycarbonate was chosen as the specimen material for two reasons. Firstly, it is a material exhibiting photoelastic effects and therefore can be used to determine the evolution of crack tip stress fields using dynamic photoelasticity. Secondly, the material exhibits rate dependent fracture mechanisms and thus would be suitable as a model material to examine the influence of changes in the fracture mechanisms on the macroscopic behavior of the specimen. The 12.7 mm deep crack was machined into the specimen with a mill cutter of 0.3 mm thickness. The root of this machined crack was scribed with a sharp razor blade to simulate a sharp crack tip. The dynamic impact loading was obtained by launching a polycarbonate projectile (50 mm diameter, 100 mm long) at speeds in the range of 25–55 m/s using an air-gun. The air-gun consisted of a reservoir, a solenoid valve and a 1.5 m long barrel, with a maximum pressure capacity of 90 psi. The speed of the projectile was measured by the interruption of a laser beam placed across the path of the projectile.

The stress field information was acquired through the methods of photoelasticity and caustics, and recorded on film using a high speed camera capable of 100,000 frames per second (fps). The high speed camera, built in-house, was a continuous access rotating mirror camera. Shuttering or framing is achieved solely by pulsing the laser light source with a pulse time of 15 ns, short enough to freeze the motion of the crack. The camera was triggered by detecting the projectile just prior to impact on the specimen and at the rate of 100,000 fps; the crack motion was followed until the crack leaves the field of view, usually for about 200 μs.

The application of the methods of photoelasticity and caustics is quite well established in dynamic fracture investigations and hence the techniques are not described here except to indicate the expected isochromatic fringe patterns under mode I and mode II for qualitative (visual) interpretation of the high speed photographs. In Fig. 2 the isochromatic fringe patterns obtained in a circular polariscope from a pure mode I and a pure mode II loading are shown. Reference to these figures will be useful in interpreting the crack tip stress state from the high speed photographs.

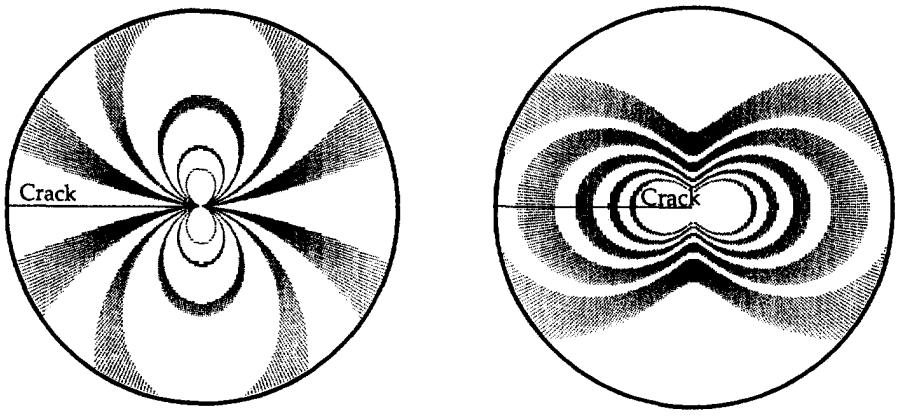

(a) (b)

Fig. 2. Isochromatic fringe patterns near a crack tip due to (a) mode I and (b) mode II loading.

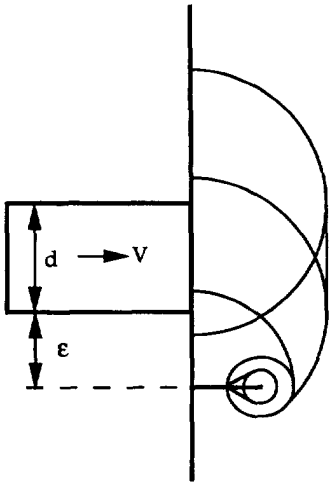

Fig. 3. Stress wave pattern emerging from impact and interaction with the crack tip; for clarity, only the dilatational waves initiating from the impact event are shown.

3. CRACK TIP STRESS FIELD

The impact of the projectile on the specimen surface generates stress waves which travel into the specimen and interact with the crack tip. A representation of the wave fronts at a time

$$t < \sqrt{\frac{l^2+(d+\varepsilon)^2}{C_d}}$$

is shown in Fig. 3. When the shear wave generated from the loading wave–crack tip interaction clears the crack tip region, a square root singular stress field governed by the dynamic stress intensity factor should be established (Freund, 1972). However, the domain over which this singular field dominates will depend on, among other things, the rate of the applied load and the magnitude of the stresses parallel to the crack tip (Ravi-Chandar and Knauss, 1987; Krishnaswamy *et al.*, 1990; Taudou *et al.*, 1992). In this particular experimental set-up, the applied loading is a compressive stress which is parallel to the crack line. Furthermore, the Poisson effect introduces a compressive stress normal to the crack tip. Thus the stress wave that approaches the crack tip is a compressive biaxial wave. For $t > 2w/C_d$, reflections from the far boundary of the specimen arrive at the crack tip further complicating the nature of the wave interaction.

In an effort to examine the development of the crack tip stress field, two identical specimens were impacted with a projectile at the same speed (28 m/s). The only difference between the two experiments was in the distance below the crack line where the specimen was impacted. The first specimen was impacted at a distance of $\varepsilon \sim 25$ mm below the crack line while the second specimen was impacted at $\varepsilon \sim 6$ mm below the crack line. This results in a large difference in the orientation of the biaxial wave as it impinges on the crack and also changes the rate of loading, due to the angular and radial variation of the amplitude of the waves traveling from the region of impact. Figures 4 and 5 show a selected sequence of high speed photographs showing the evolution of the dynamic isochromatics in these two specimens. It is clear from the frame labeled 0 μs in Fig. 4 that the impact has already occurred and that a wave front is just beginning to enter the field of view of the high speed camera. After 20 μs, the wave front has arrived at the crack tip and the beginning of the scattering of the wave from the crack tip can be observed. However, the isochromatic fringe patterns do not indicate the typical loops around the crack tips suggested in Fig. 2 for a pure mode I or mode II state; at this time, the shear wave generated from the crack tip has traveled about 10 mm from the crack tip. It takes a further 20 μs before the crack tip isochromatic pattern resembles a predominantly mode II type of singular field as can be verified by comparing the frame at 40 μs with Fig. 2(b). However, the mode II type field

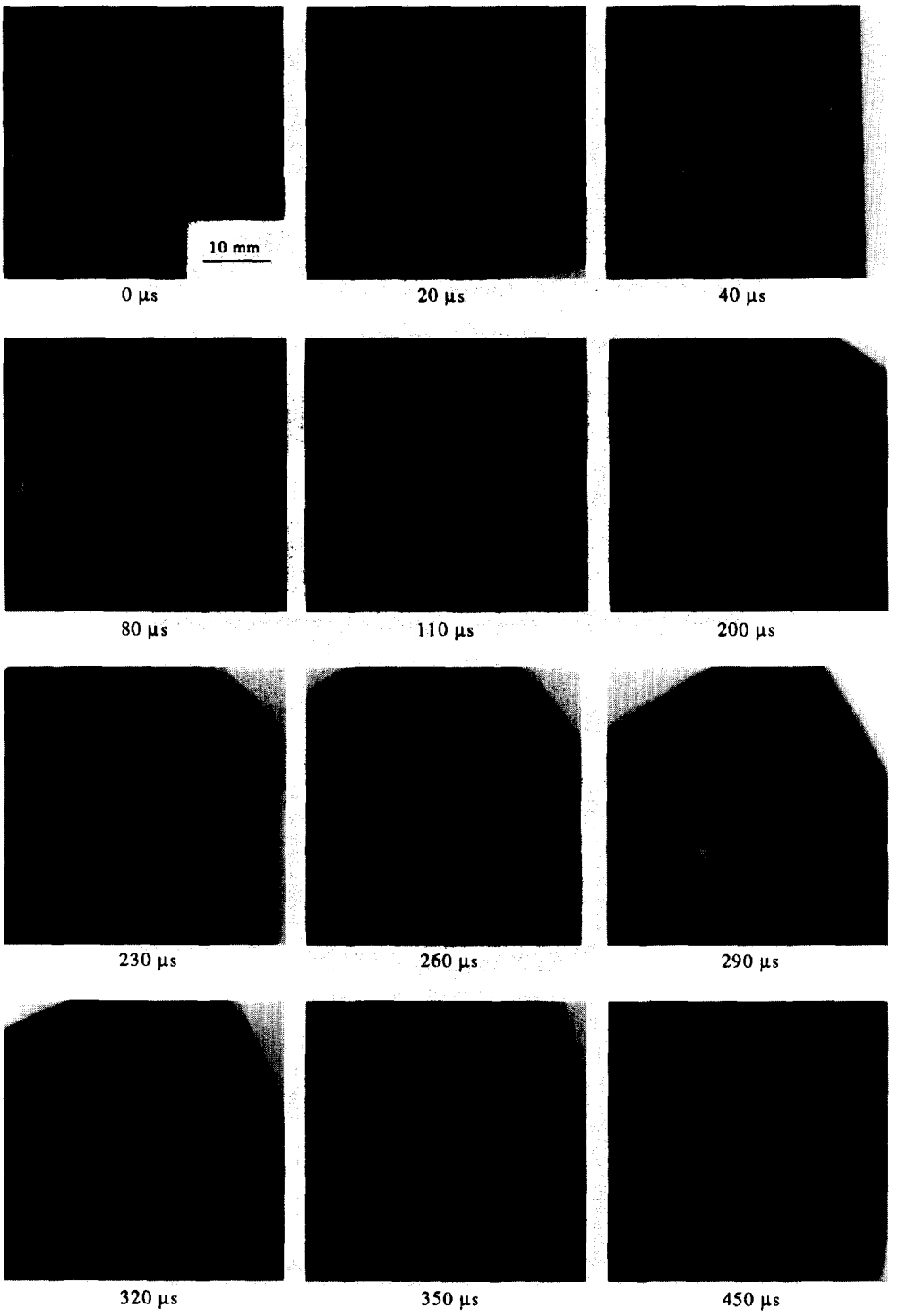

Fig. 4. Selected high speed photographs showing isochromatic patterns; projectile speed = 28 m/s, ε = 25 mm.

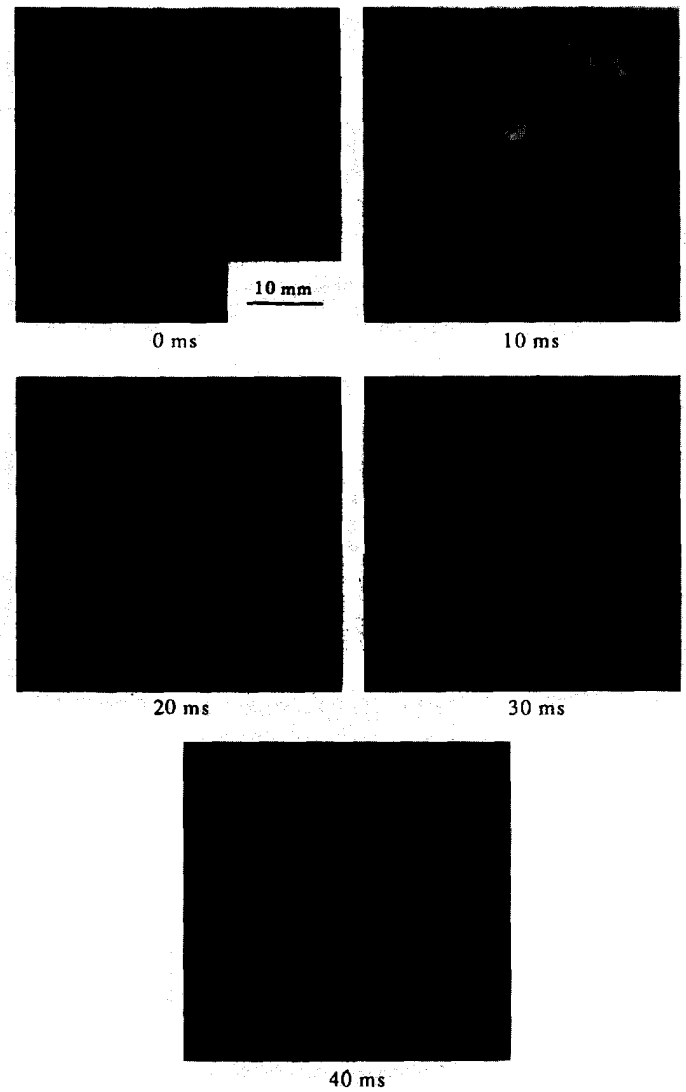

Fig. 5. Selected high speed photographs showing isochromatic patterns; projectile speed = 28 m/s, $\varepsilon = 6$ mm.

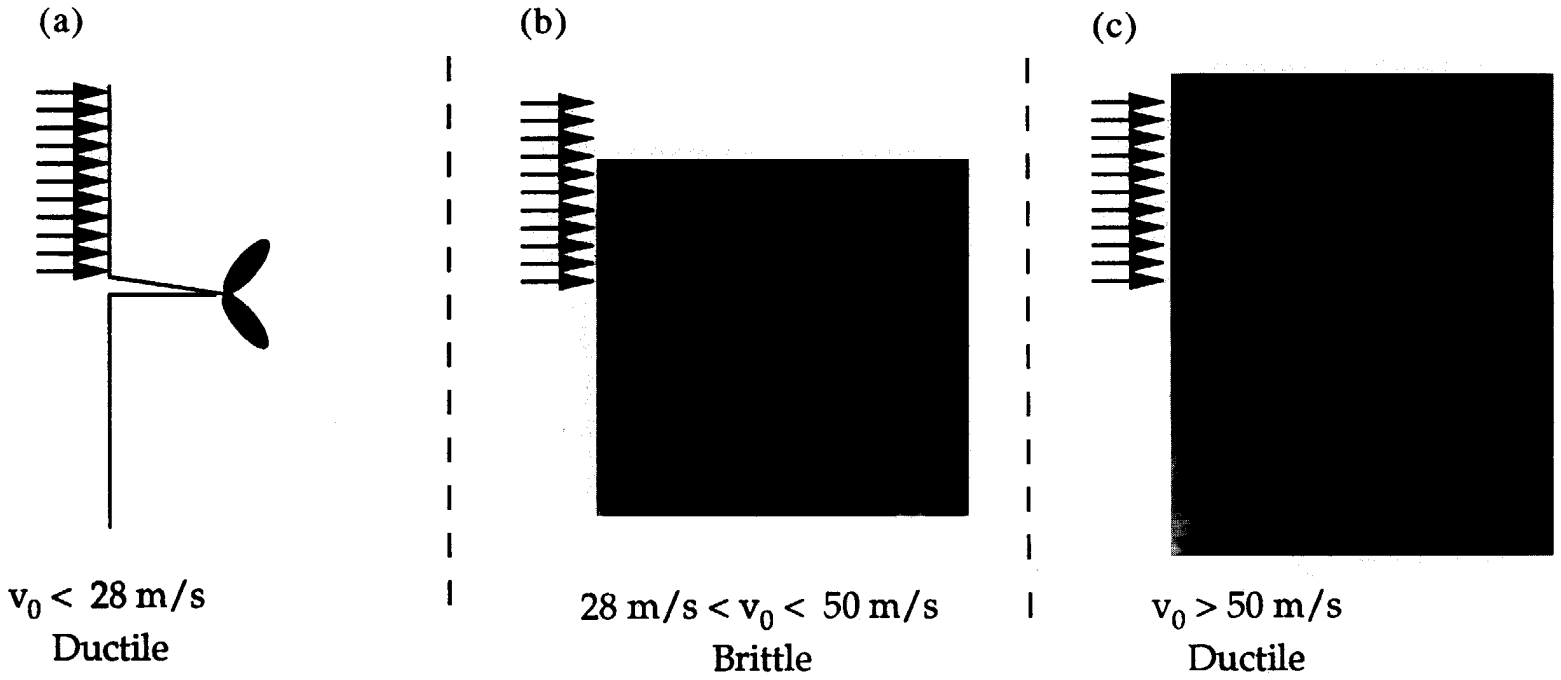

Fig. 6. Failure mode transitions in polycarbonate as a function of projectile speed.

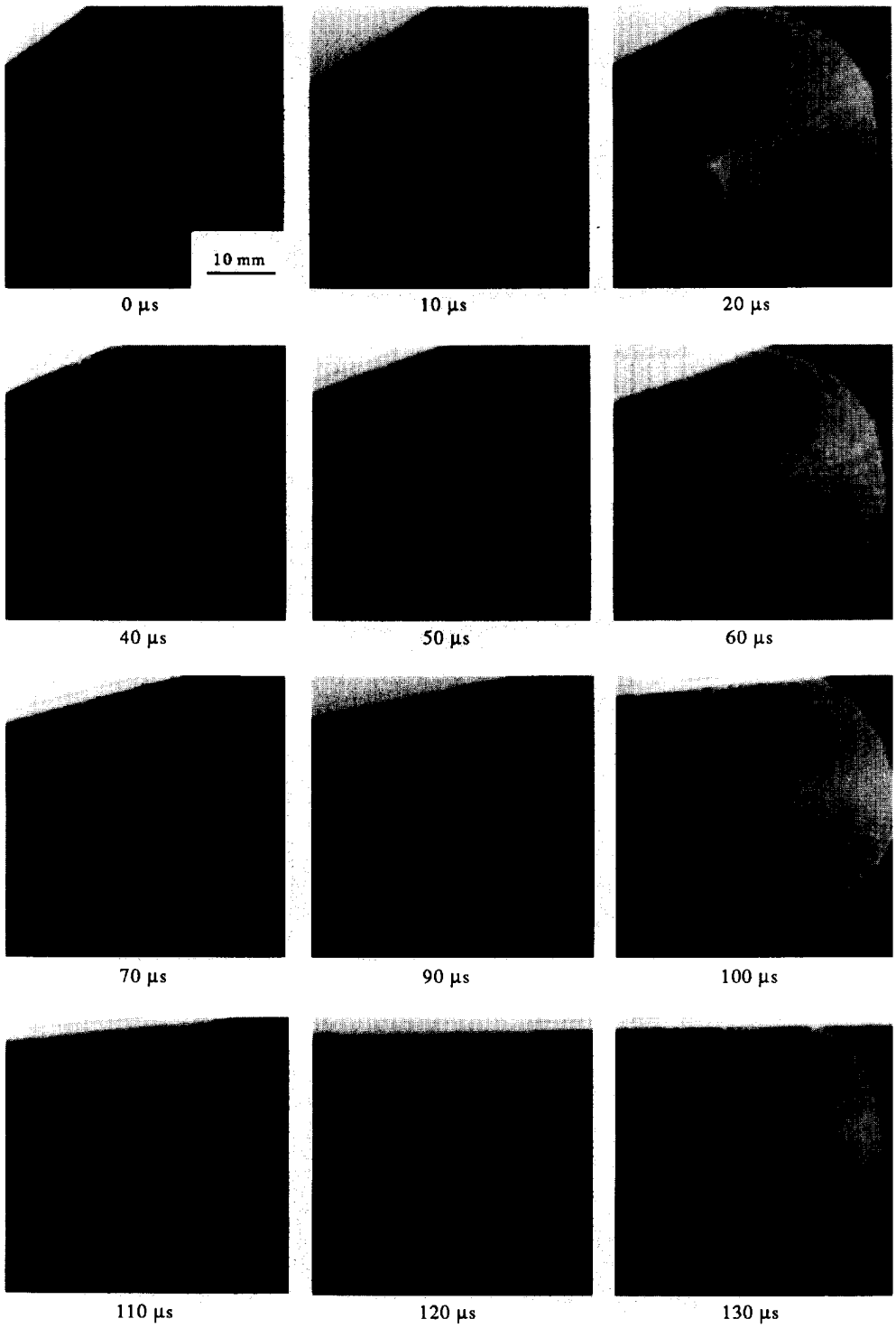

Fig. 7. Selected high speed photographs showing caustic patterns; projectile speed = 32 m/s, $z = 3$ mm.

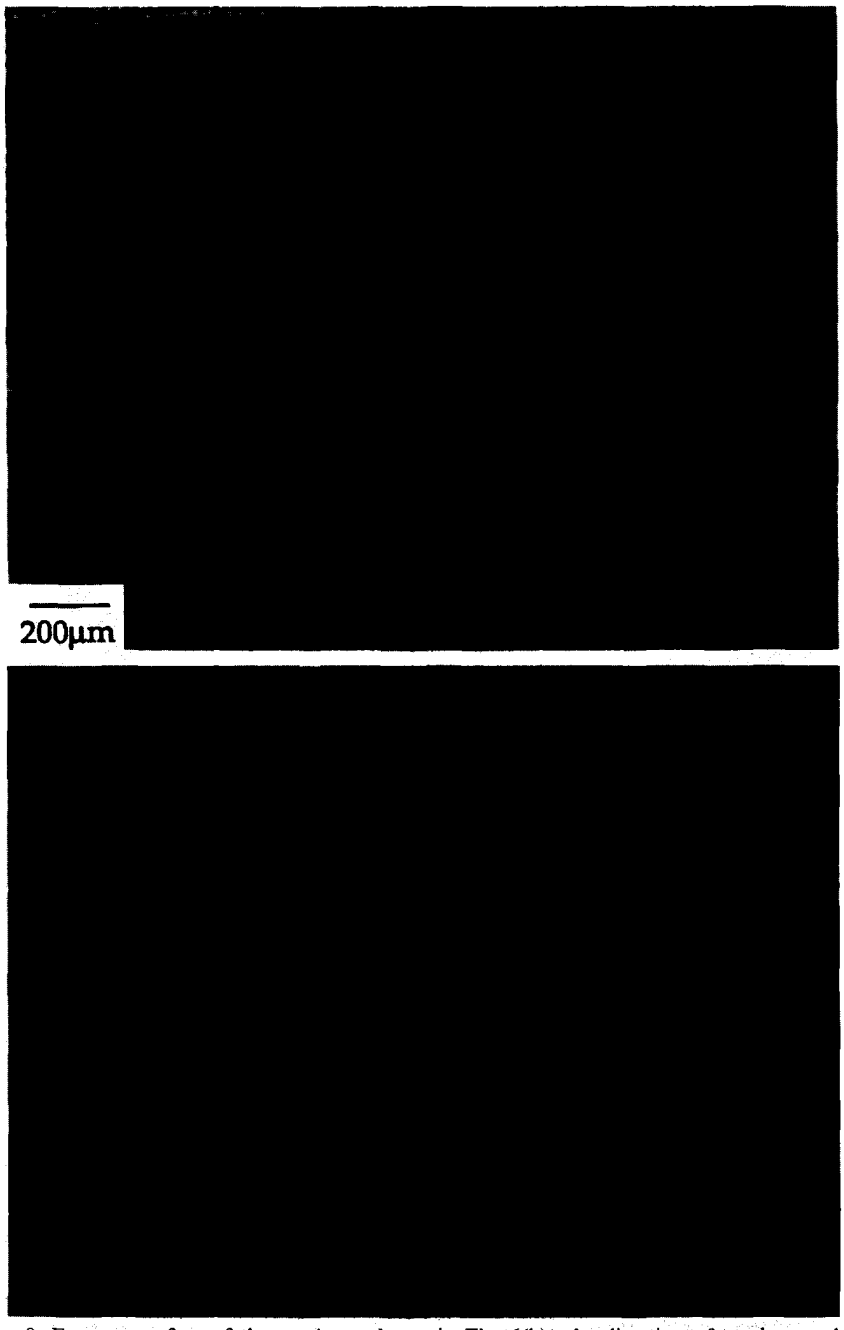

Fig. 8. Fracture surface of the specimen shown in Fig. 6(b); the direction of crack growth is indicated by the arrow.

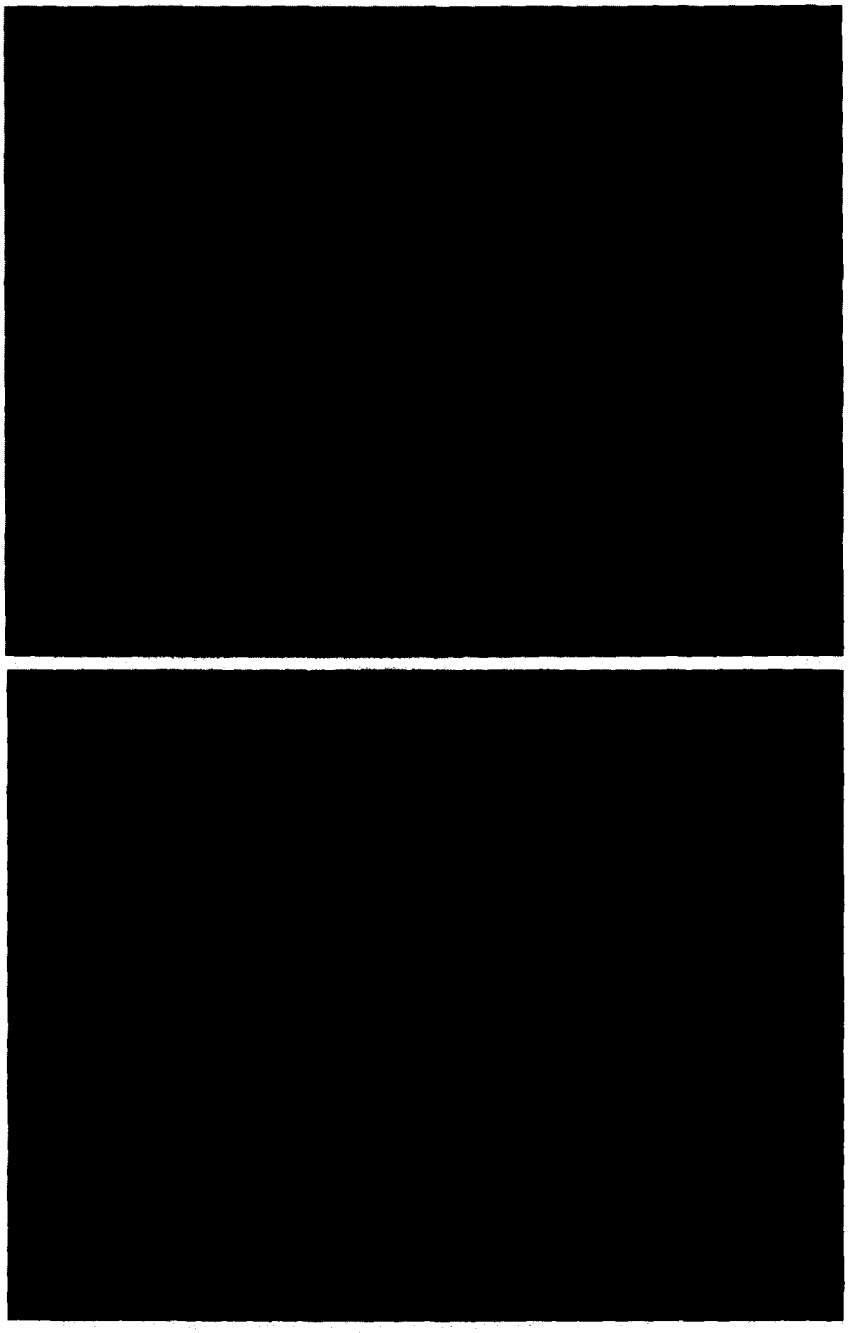

Fig. 9. Fracture surface of the specimen shown in Fig. 6(c); the direction of crack growth is indicated by the arrow.

does not persist for very long; as can be seen from the continuing sequence of frames, at 80 μs and 110 μs after impact, the isochromatics suggest that a stress intensity factor dominated mixed-mode stress field exists near the crack tip, with a larger mode I component. At about 200 μs the stress wave reflected from the far boundary of the specimen arrives at the crack tip and alters the stress field drastically; the isochromatics do not show any resemblance to the square root singular field shown in Fig. 2. The high density of the isochromatics points to the existence of a very large shear stress gradient in the neighborhood of the crack tip, but the crack tip does not appear to govern the stress field with its typical square root singular behavior. At later times, the emergence of the looping isochromatics indicates the development of the singular field. The loading amplitude in this test was not sufficient to initiate the crack. Thus, at very long times (~ 500 μs), the crack experiences a mode I loading similar to the observations of Mason *et al.* (1992), but the crack is stationary.

In the second experiment, with the impact occurring at a distance of $\varepsilon \sim 6$ mm from the crack line, the biaxial loading wave arrives at the crack tip quickly. The development of the crack tip stress field can be seen from the high speed photographs in Fig. 5. In the frame arbitrarily labeled 0 μs, the loading wave arrives in the field of view of the high speed camera; 10 μs later, the wave front has traveled a further 20 mm and has encountered the crack tip. The scattering of the wave front about the crack is evident from this photograph. However, the fringe loops, similar to the square root singular field observed in the previous experiment, do not emerge in this case. Note also that the density of the isochromatic fringes is much greater than in Fig. 4 indicating that the shear stress gradients are indeed quite large. The region near the crack tip is obscured by a pseudo-schlieren effect;† thus, if there exists a square root singular field, it lies inside the region that is dark. At 40 μs, the obscured region is roughly circular with a radius of about 3 mm; the isochromatics are not of the loop type shown in Fig. 2, but closer to the "frontal lobe" type of fringes identified by Taudou *et al.* (1992). In this experiment, as in the first, the loading was insufficient to initiate the crack, but rather a large plastically deformed zone was developed.

Two main results of this exploration of the stress field are as follows. Firstly, while a more detailed exploration of the stress field is necessary, it is clear that the domain over which the square root singular field dominates depends on the rate at which the loading is applied, in agreement with similar observations made earlier with respect to mode I loading. Secondly, the mode mixity at the crack tip varies as a function of time and the direction of crack initiation will depend on the time at which initiation occurs. Thus, in interpreting the experimental results from this kind of loading arrangement, it is necessary to follow the evolution of the local conditions at the crack tip. We now turn to an examination of the failure modes resulting from the asymmetric impact loading on the edge cracked plate.

4. FAILURE MODE TRANSITIONS

Polycarbonate is a thermoplastic polymer with a molecular structure that consists of a bisphenol A component and a carbonate component; the bisphenolic component gives a high glass transition temperature of about 150°C while the carbonate component provides a high rotational mobility resulting in a capacity to shear yield. Thus, at room temperature at low to moderate rates of loading, as is available from standard testing machines, polycarbonate exhibits a ductile fracture behavior; as the loading rate is increased, a ductile to brittle fracture transition occurs (Parvin and Williams, 1975) which is similar to such transitions observed in metals. In the present experiments using the asymmetric impact of the edge cracked plate, in addition to this ductile to brittle transition, at higher rates of loading a brittle to ductile fracture transition with increasing loading rates was observed. It must be observed that, as the loading rate was increased, the crack tip constraint could not be maintained at the same level due to the nature of the biaxial loading wave that is

† The diameter of the rotating mirror of the high speed camera is about 13 mm and therefore light rays that deviate to large angles are effectively cut off from the film; thus the mirror plays a role similar to a knife edge in a schlieren set-up and these light rays do not reach the film plane.

generated. The ductile to brittle to ductile transition and the micromechanisms responsible for these transitions in polycarbonate are examined below.

A number of experiments were performed with the asymmetric impact loading arrangement shown in Fig. 1(c). The velocity of impact V was gradually increased from about 20 m/s to about 55 m/s. A simple one-dimensional estimate of the magnitude of the applied-load ($\sigma = \rho c V/2$) indicates that the applied compressive stress is in the range of 25–75 MPa, lower than the uniaxial compressive yield stress of about 100 MPa.† In all these experiments the projectile impact was at $\varepsilon = 3$ mm above the crack line. Figure 6 provides a summary of the observed crack response to the impact loading in this range. At impact velocities less than about 30 m/s, the stresses near the crack were not elevated sufficiently to initiate the crack. Also, at this impact velocity, the loading rate was sufficiently low to generate inelastic deformation near the crack indicating that the loading conditions were below the ductile to brittle transition range. Thus, a very large inelastically deformed zone appears in this range of impact speeds [see Fig. 6(a)].

As the impact speed is increased to the range of 30–50 m/s, brittle crack initiation occurs long before the waves reflected from the far boundary of the specimen arrive at the crack tip.‡ The angle of crack initiation is about 66°, as shown in Fig. 6(b). This angle is close to the location of the maximum circumferential stress calculated by Lee and Freund (1990) and indicates that the crack propagated along the direction of local symmetry. This particular experiment was examined using the optical method of caustics and the corresponding high speed photographs are shown in Fig. 7. The asymmetry of the caustic curve about the crack line indicates the presence of both a mode I and mode II component. The crack propagates nearly along a straight line at a velocity of about 600 m/s; this velocity is in the same range observed under mode I loading conditions examined earlier (Taudou *et al.*, 1992). The corresponding fracture surface appears to be mirror-like (specularly reflecting) and flat all across; shear lips are absent indicating that this fracture is truly a brittle fracture. However, under high magnification, the crack surface reveals a periodic banded structure, similar to that observed by Green and Pratt (1974), Fineberg *et al.* (1992) and Washabaugh and Knauss (1993) in polymethylmethacrylate (PMMA). Figure 8 shows two magnified views of the fracture surface, where the direction of crack propagation is indicated by the arrow. The periodic banded structure is suggested to be the result of the craze dominated mechanism of fracture. In comparison with PMMA, the size scale of the bands is very small; while the periodic bands in PMMA are in the millimeter scale, the bands in polycarbonate are on the order of 30 μm. The apparent correlation between the size of the bands and the stress intensity factor used to generate them, which was demonstrated by Washabaugh and Knauss (1993) over a wide range of time scales from fatigue to fast fracture, does not appear to hold in this particular example and needs to be investigated further. However, the periodic surface texture and the kinking angle of $\sim 66°$ can be taken as evidence that the crack propagated by a mechanism (such as crazing) governed by the normal stress.

As the impact velocity is increased above ~ 50 m/s, the craze dominated fracture mechanism is suppressed and an entirely new cracking mechanism becomes operative; as shown in Fig. 6(c), the crack extends straight along the original crack line for about 10 mm and then arrests! Good quality high speed photographs were not obtained from this experiment, but post-mortem examination of the fracture specimen provides a qualitative indication of the fracture mechanism; further experiments are currently underway to examine the problem quantitatively. Firstly, the fact that the crack arrested at a higher impact energy indicates that the present mechanism for crack growth consumes more energy than the craze dominated fracture observed in the brittle range. Secondly, since the crack growth was along the original crack line and not along the direction of maximum circumferential stress, the crack growth must be governed by the maximum shear stress. This

† Post-mortem examination of the broken plates revealed very little permanent deformation at the impact location.

‡ In fact, there is another velocity range in which the kinked crack initiation is promoted by the increase of stresses due to the arrival of the reflected waves; the resulting crack exhibits shear lips towards the ends and a flat fracture in the middle of the crack plane. This is currently being explored further and will be reported elsewhere.

observation of crack extension along the line of maximum shear is similar to that observed by Kalthoff (1988) in steels where shear localization occurred near the crack tip. Magnified views of the fracture surface are shown in Fig. 9. From an examination of the fracture surface, and comparing it to the fracture surface for the brittle opening mode cracking in Fig. 8, it can be concluded that the micromechanism governing fracture is clearly not crazing. Also, extensive dimpling and drawing evident on the fracture surface in Fig. 9 implies a ductile fracture mechanism was operative; in Fig. 9(b) stretching of the polymer ligaments can be clearly seen indicating that softening of the material might have occurred perhaps by the heating due to the deformation. Since the normal stress on the plane where this cracking occurred can be shown to be compressive, clearly the fracture was driven by shear. Thus, the fracture mode has undergone a transition from a brittle to a ductile mechanism with increase in the rate of loading! However, the constraint has also changed; it is noted that as the speed of the projectile increases, the amplitude of the biaxial compressive stress also increases and prevents the opening mode of cracking from propagating at the 66° angle, as was predicted by Broberg (1983). There remains the question of whether the shear strain localized along the line ahead of the crack prior to shear cracking along this plane. To resolve this issue, further studies on the rate dependent plastic response of polycarbonate are required and are currently being explored. We also note the similarities in the fracture behavior of the high strength steel investigated by Kalthoff (1988) and the polycarbonate investigated here; while the micromechanisms responsible for the fracture are very different, macroscopically, the response appears to be similar. Of course, the impact velocities at the transition of the failure modes and the energy absorbed in the failure process are different. It would appear that as long as two different mechanisms of fracture, one dominated by maximum normal stress and the other dominated by maximum shear stress, are available, the nature of the application of the load would select the energetically favorable mechanism and one should be able to induce such failure mode transitions in many different materials, reinforcing Broberg's conclusions. This is also reinforced by recent numerical modeling by Needleman and Tvergaard (1994) who considered an elasto–viscoplastic constitutive relation for a porous plastic solid including nucleation and growth of voids and thermal softening of the plastic response; their results indicate similar failure mode transitions.

5. CONCLUSION

The failure behavior of edge cracked plates due to asymmetrical impact loading was investigated using polycarbonate, a thermoplastic polymer. The development of the crack tip stress field was shown to be quite complex; it was also shown that the square root singular dynamic crack tip stress field does not establish its dominance over a significant domain near the crack tip at all times. Failure mode transitions were induced in the polymer capable of crazing as well as shear yielding by appropriately varying the rate of loading and the crack tip constraint. At very low rates of loading, a diffuse plastic zone was observed near the crack tip without initiation of the crack; at moderate rates of loading, a ductile to brittle transition in the failure mode was observed, with crazing being the mechanism of crack growth. Finally at very high rates of loading, a brittle to ductile transition was observed, with the crack growth being governed by a shear deformation mechanism. These observations are similar to the failure mode transitions observed by Kalthoff (1988) in a high strength steel.

REFERENCES

Broberg, B. (1983). On crack paths. In *Proc. NSF-ARO Workshop on Dynamic Fracture* (Edited by W. G. Knauss, K. Ravi-Chandar and A. J. Rosakis), pp. 140–155. California Institute of Technology, Pasadena, CA.

Cotterell, B. and Rice, J. R. (1980). Slightly curved or kinked cracks. *Int. J. Fract.* **16,** 155–169.

Erdogan, F. and Sih, G. C. (1963). On the crack extension in plates under plane loading and transverse shear. *J. Basic Engng* **85D,** 519–527.

Fineberg, J., Gross, S. P., Marder, M. and Swinney, H. L. (1992). Instability in the propagation of fast cracks. *Physical Rev. B* **45,** 5146–5154.

Freund, L. B. (1972). Crack propagation in an elastic solid subjected to general loading—II. Non-uniform rate of extension. *J. Mech. Phys. Solids* **20,** 141–152.

Green, A. K. and Pratt, P. L. (1974). Measurements of dynamic fracture toughness of polymethylmethacrylate by high speed photography. *Engng Fract. Mech.* **6,** 71–80.

Kalthoff, J. F. (1988). Shadow optical analysis of dynamic shear fracture. *Optical Engng* **27,** 835–840.

Kalthoff, J. F. (1990). Transition in the failure behavior of dynamically shear loaded cracks. *Appl. Mech. Rev.* **43,** S247–S250.

Krishnaswamy, S. and Rosakis, A. J. (1991). On the extent of the dominance of asymptotic elastodynamic crack tip fields. Part I: an experimental study using bifocal caustics. *J. Appl. Mech.* **58,** 87–94.

Lee, Y. J. and Freund, L. B. (1990). Fracture initiation due to asymmetric impact loading of an edge cracked plate. *J. Appl. Mech.* **57,** 104–111.

Mason, J. J., Lambros, J. and Rosakis, A. J. (1992). The use of a coherent gradient sensor in dynamic mixed-mode fracture mechanics experiments. *J. Mech. Phys. Solids* **40,** 641–661.

Needleman, A. and Tvergaard, V. (1994). Analysis of dynamic ductile crack growth under shear loading (to appear in *Int. J. Solids Structures*).

Parvin, M. and Williams, J. G. (1975). Ductile–brittle fracture transitions in polycarbonate. *Int. J. Fract.* **11,** 963–972.

Ravi-Chandar, K. and Knauss, W. G. (1984). An experimental investigation into dynamic fracture—IV: On the interaction of stress waves with propagating cracks. *Int. J. Fract.* **26,** 189–200.

Ravi-Chandar, K. and Knauss, W. G. (1987). On the characterization of the transient stress field near the tip of a crack. *J. Appl. Mech.* **54,** 72–78.

Taudou, C., Potti, S. and Ravi-Chandar, K. (1992). On the dominance of the dynamic crack tip stress field under high rate loading. *Int. J. Fract.* **56,** 41–59.

Washabaugh, P. D. and Knauss, W. G. (1993). Nonsteady periodic behavior in dynamic fracture of PMMA. *Int. J. Fract.* **59,** 187–197.